Article published online: 2023-09-12

Design, Synthesis, and Neuroprotective Effects of Novel Cinnamamide-Piperidine and Piperazine Derivatives

Jia-Yi Li[1,2,#] Xin-Yan Peng[2,#] Yi-Lei Huang[2] Ling Jiang[2] Jian-Qi Li[2] Xue-Zhi Yang[3] Qing-Wei Zhang[1,2*]

[1] School of Chemistry and Chemical Engineering, Shanghai University of Engineering Science, Shanghai, People's Republic of China
[2] Shanghai Institute of Pharmaceutical Industry Co., Ltd., China State Institute of Pharmaceutical Industry, Shanghai, People's Republic of China
[3] Department of Neurology, The First Affiliated Hospital of Wenzhou Medical University, Wenzhou, People's Republic of China

Address for correspondence Qing-Wei Zhang, PhD, Shanghai Institute of Pharmaceutical Industry Co., Ltd., 285 Gebaini Road, Shanghai 201203, People's Republic of China (e-mail: sipiqingwei@163.com).

Pharmaceut Fronts 2023;5:e132–e140.

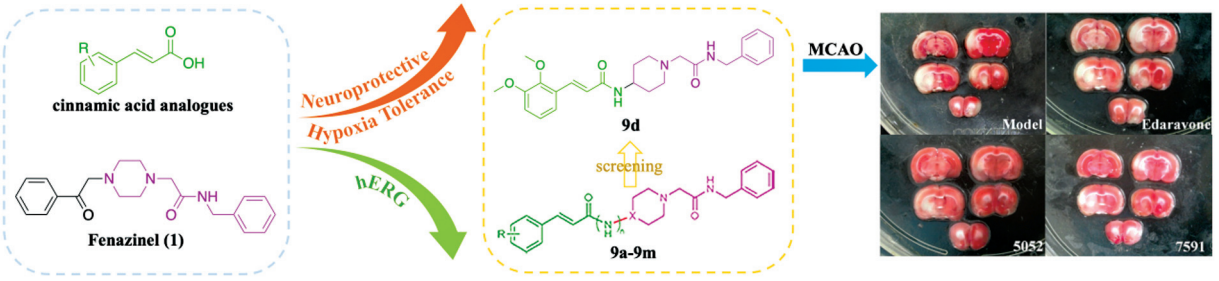

Abstract

In our previous studies, Fenazinel has shown good neuroprotective effects; however, when Fenazinel entered phase 1 clinical trials, it was associated with certain side effects. This study aimed to explore novel neuroprotective agents with higher potency and lower toxicity. Evidence suggested that cinnamic acid and its analogs may serve as promising lead compounds for stroke treatment. In this study, a series of Fenazinel derivatives were first synthesized with potential neuroprotective effects with fragments including cinnamic acid and its analogs as key functional groups. The methyl thiazolyl tetrazolium assay was performed to assess the neuroprotective effects of the compounds in glutamate-induced neurotoxicity in SH-SY5Y cells. The hERG binding assay was conducted to assess drug-induced QT prolongation or other cardiotoxicity. The neuroprotective activity of the most potent compound *in vivo* was tested through the survival time of mice under the hypoxic condition and a middle cerebral artery occlusion model. Our data suggested that among those derivatives, compound **9d**

Keywords
- stroke
- cinnamic acid
- derivatives
- hERG
- neuroprotective

[#] *These authors contributed equally to this work.*

received
October 28, 2022
accepted
August 10, 2023
article published online
September 12, 2023

DOI https://doi.org/10.1055/s-0043-1774288.
ISSN 2628-5088.

Georg Thieme Verlag KG, Rüdigerstraße 14, 70469 Stuttgart, Germany

exhibited potent neuroprotective activity *in vitro* comparable to Fenazinel at the test concentrations. Significantly, **9d** exhibited weak hERG inhibitory activity, showing moderate activities in both hypoxia-tolerant and MCAO models *in vivo*. Given the above, **9d** has the potential for the treatment of stroke and could be considered a lead neuroprotective agent for further development.

Introduction

Stroke ranks as the second most common cause of death and a leading cause of disability worldwide.[1] It can be categorized into ischemic stroke and hemorrhagic stroke, with the former being more prevalent, accounting for approximately 80% of all stroke cases.[2] Currently, tissue plasminogen activator remains the only Food and Drug Administration-approved drug for treating ischemic stroke. Edaravone, a free-radical scavenger, has been only approved for use in the treatment of acute ischemic stroke in Japan and China. Therefore, the identification and validation of novel therapeutic strategies for stroke is of paramount importance.[3] In previous studies, we designed and synthesized a series of dicarbonylalkyl piperazine derivatives to explore their neuroprotective properties.[4–6] Specifically, compound **1** (Fenazinel, ►**Fig. 1**, also named SIPI5052/5052)[7–10] and compound **8o**[4] demonstrated promising neuroprotective effects both *in vitro* and *in vivo*. In 2006, Fenazinel entered phase 1 clinical trials in China as a novel neuroprotective agent. However, during clinical trials, Fenazinel's administration was associated with certain side effects: elevated serum phosphocreatine kinase activity in two patients, and potential premature atrial contractions in another patient. As a result, we conducted a comprehensive evaluation of Fenazinel's pharmacological profile to determine any significant off-target activity or metabolic disorders associated with the compound. Follow-up studies revealed that Fenazinel had mild activity in the hERG patch-clamp K^+ channel binding assay, with an IC_{50} value of 8.64 µmol/L. Meanwhile, its major metabolite **M1** (**3**) in the human body had a hERG IC_{50} value of 0.43 µmol/L, suggesting **M1** might contribute to drug-induced QT prolongation or other cardiotoxicity. Given the increasing regulatory emphasis on drug-induced QT prolongation,[11] we believe it is essential to mitigate the hERG activity of these compounds through structural modification.

In recent years, traditional Chinese medicine has gained extensive acceptance for treating nervous system diseases.[12–14] Cinnamic acid (3-phenylprop-2-enoic acid) and its analogues (ferulic acid,[15] sinapic acid,[16,17] *p*-methoxycinnamic acid,[18] etc.) are prolific in plants. These compounds display an array of pharmacological activities, including antioxidant properties, neuroprotection, antithrombotic effects, angiogenesis promotion, and vascular protective capacities.[19–21] These attributes suggest that cinnamic acid and its analogues could serve as promising lead compounds for stroke treatment.

In this study, we sought to mitigate potential cardiac risks by replacing groups within the structures of Fenazinel or **M1** with fragments from cinnamic acid and its analogues, thereby creating novel cinnamamide-piperidine and piperazine derivatives. We anticipated that the integration of these natural active ingredients with Fenazinel would generate a synergistic effect in neuroprotection, while simultaneously mitigating the risk of cardiotoxicity.

Results and Discussion

Chemistry

The synthesis of the analogues, designated as **9a**–**m**, was obtained following the processes depicted in various schemes. As outlined in ►**Scheme 1**, different substituted benzyl/acetaldehyde **4a**–**l** reacted with malonic acid via the Perkin reaction to afford intermediate **5a**–**l**, and then coupled intermediate **7** with triethylamine in the presence of HBTU (*O*-(benzotriazol-1-yl)-*N*,*N*,*N*′,*N*′-tetramethyl-uronium hexafluorophosphate)

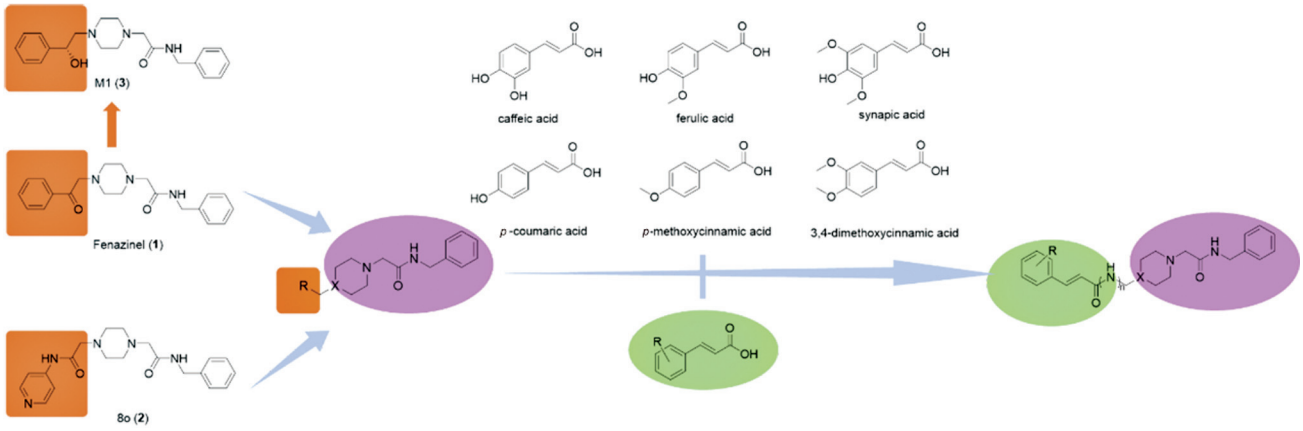

Fig. 1 Design of cinnamamide-piperidine and piperazine derivatives.

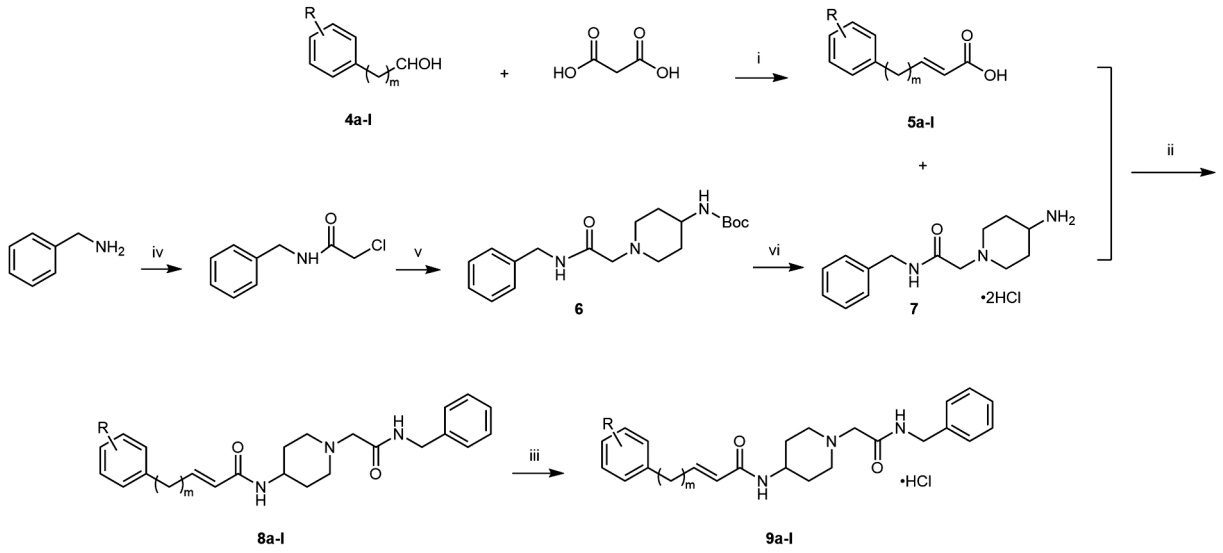

Scheme 1 Synthesis of compounds **9a–l**. Reagents and conditions: i) piperidine, pyridine, reflux, 5 hours; ii) HBTU, TEA, DMF, r.t., 8 hours; iii) HCl/EA; iv) 2-chloroacetyl chloride, K_2CO_3, DCM, 40°C, 4 hours; v) K_2CO_3, KI, MeCN, 40°C, 4 hours; vi) HCl/EA, 1 hour.

to produce compounds **8a–l**. Finally, the target compound **9a–l** was obtained by a salification reaction with hydrochloric acid. The analogues are listed in ►**Table 1**.

The synthesis of **9m** is shown in ►**Scheme 2**. A nucleophilic substitution of *tert*-butyl piperazine-1-carboxylate with *N*-benzyl-2-chloroacetamide generated intermediate **10** and aqueous HCl-mediated deprotection afforded intermediate **11**, which coupled with 4-methoxycinnamic acid provided compound **12**. Ultimately, the target compound **9m** was obtained by a salification reaction with hydrochloric acid.

Biological Activity

To test the potential neuroprotective activities of these target compounds, a preliminary screening was performed investigating neuroprotection on impairment induced by glutamic acid deprivation in SH-SY5Y cells, as evaluated by methyl thiazolyl tetrazolium (MTT) assay. The results are shown in ►**Table 1**. Six compounds (**9a**–**b**, **9i, 9k**–**m**) showed slight neuroprotection capacity at two test concentrations (1 and 10 μmol/L), with cell survival rates ranging from 50.24 to 57.83%. Two compounds (**9c** and **9d**) exhibited moderate to good neuroprotective effect at two levels of concentration in comparison with Fenazinel (**9c**: 60.09% and 57.41%; **9d**: 56.53% and 59.65% viable rate at 1 and 10 μmol/L, respectively). The compound **9j** exhibited weaker activity at the low concentration of 1 μmol/L, but showed better protective activity than the positive compound Fenazinel at the high concentration of 10 μmol/L.

The preliminary structure–activity relationship (SAR) showed the neuroprotective activities of the derivatives (**9c** and **9d**) with two methoxyl groups on the benzene ring were better than those of mono-substituted (**9a** and **9h**) and trisubstituted derivatives (**9b**). The length of the left carbon chain had no significant effect on the activity of the compound (**9k** and **9l**). Meanwhile, the piperidine derivative (**9m**) and piperazine derivative (**9a**) had no significant difference in activity.

Evidence suggested that neuroprotective agents may be cytotoxic at high concentrations.[22–25] To further evaluate the potency and toxicity of compounds, we selected the most potent compounds **9c** and **9d** to test their neuroprotection capacity in high concentrations (10, 20, 50, and 100 μmol/L), using Fenazinel as the positive control group. According to the results of the MTT assay (►**Fig. 2**), different concentrations of all compounds' solutions exhibited different degrees of damage toward SH-SY5Y cells, and with the increase in concentration, the survival rate of SH-SY5Y cells decreased gradually, showing a dose–effect relationship. Among them, compound **9d** showed similar cell viability to Fenazinel at four test concentrations, which was worth further investigation as a novel neuroprotective agent.

Based on the above analysis, compound **9d** was further evaluated in hERG binding assay and hypoxia tolerance model in mice (►**Table 2**). Compound **9d** showed weak inhibition in the hERG binding assay with an IC_{50} value of 24.61 μmol/L and almost threefold increased value compared with Fenazinel, which indicated that the possibility of compound **9d** causing drug-induced QT prolongation was lower. Hypoxia tolerance assay *in vivo* showed that compound **9d** could prolong the survival time of mice under the hypoxic condition at a dose of 20 mg/kg compared with the control group and was slightly weaker than the Fenazinel group. Therefore, it can be considered as a new lead compound for further development in specific tests for a potential neuroprotective agent.

To investigate the activity of **9d** (also named SIPI**7591/7591**) *in vivo*, we tested its potential anti-ischemic stroke effects on a rat model of middle cerebral artery (MCA) occlusion (MCAO). Then MCAO rats were injected intraperitoneally with compound **7591** (5 mg/kg), Fenazinel/**5052** (5 mg/kg), and

Table 1 Preliminary *in vitro* neuroprotective activity of the targeted compounds of **9a–m**

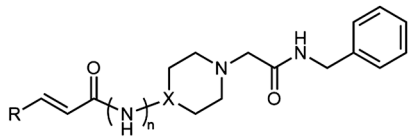

Compd.	R	*n*	X	Glu deprivation test, survival rate (%)	
				1 μmol/L	10 μmol/L
9a	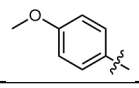	1	CH	54.45 ± 0.23	50.24 ± 0.20
9b	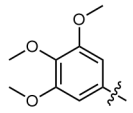	1	CH	51.32 ± 0.38	51.14 ± 0.98
9c	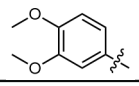	1	CH	60.09 ± 1.61	57.41 ± 7.20
9d	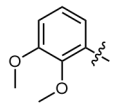	1	CH	56.53 ± 3.52	59.65 ± 0.83
9e	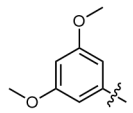	1	CH	57.19 ± 0.60	49.19 ± 0.93
9f	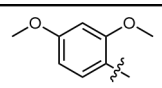	1	CH	46.37 ± 0.53	57.64 ± 2.45
9 g	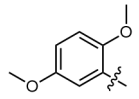	1	CH	56.04 ± 5.68	49.31 ± 1.89
9h	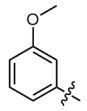	1	CH	48.06 ± 1.38	52.04 ± 6.44
9i	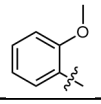	1	CH	55.98 ± 1.08	52.47 ± 1.61
9j	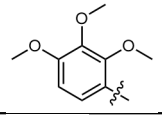	1	CH	50.69 ± 0.22	65.21 ± 1.61
9k		1	CH	54.47 ± 1.32	57.03 ± 4.01
9l	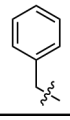	1	CH	54.45 ± 2.47	50.67 ± 2.43
9m	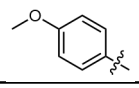	0	N	57.83 ± 1.15	55.40 ± 2.75
Fenazinel	–	–	–	56.27 ± 0.86	56.11 ± 1.01
Vehicle (Damage model)				50.58 ± 1.13	

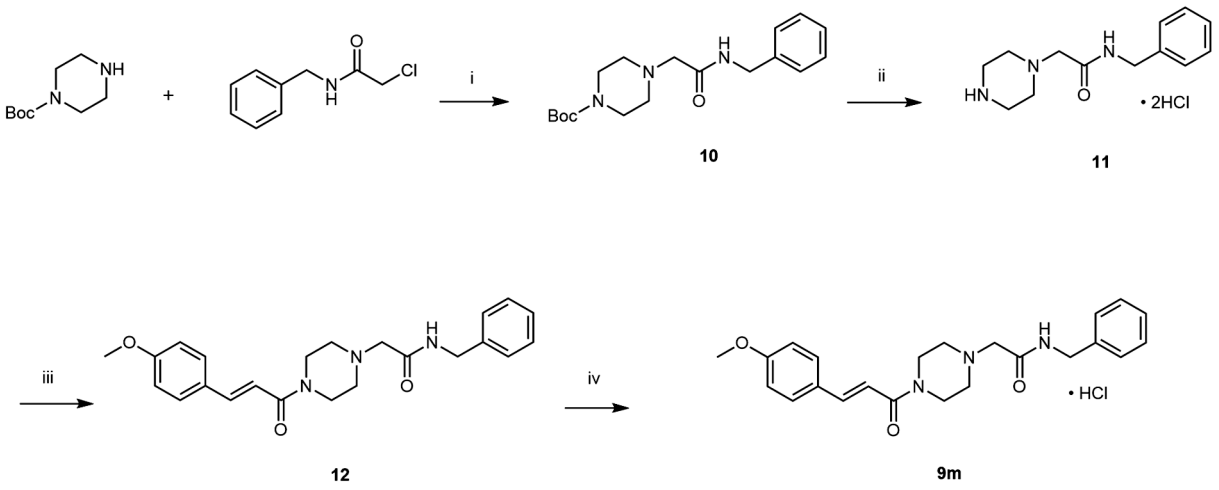

Scheme 2 Synthesis of compound **9m**. Reagents and conditions: i) K_2CO_3, KI, MeCN, 40°C, 6 hours; ii) HCl/EA, MeOH, r.t., 36 hours; iii) 4-methoxycinnamic acid, HBTU, TEA, DMF, r.t., 8 hours; iv) HCl/EA, 1 hour.

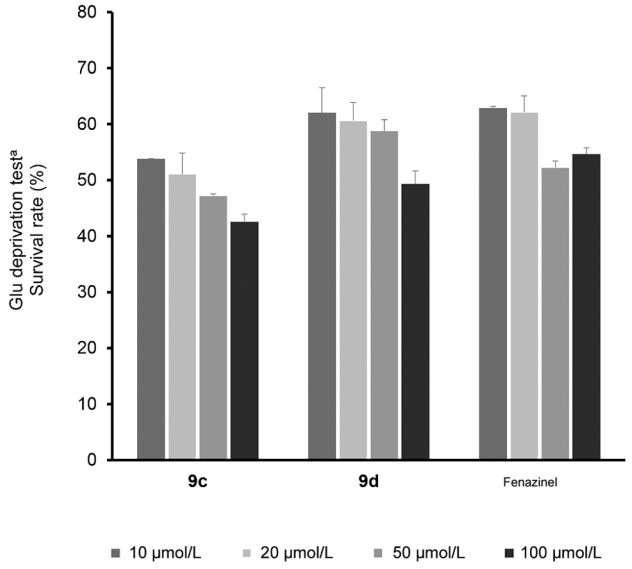

Fig. 2 Further studies on the *in vitro* neuroprotective activity of the most potent compounds **9c** and **9d** at high concentrations.

Edaravone (5 mg/kg), respectively. The results (►**Fig. 3**) showed that the positive control drug Fenazinel significantly reduced the area of cerebral infarction. Meanwhile, compound **9d** exhibited a trend toward reducing the infarct area, although the difference was not statistically significant. While we did not observe significant neuroprotective effects of Edaravone groups in this experiment. Further, *in vivo* experiments on neuroprotective effects are underway.

Conclusion

Based on the SAR analysis of Fenazinel and its toxic metabolite **M1**, we designed and synthesized a series of novel cinnamamide-piperidine and piperazine derivatives. The results showed that most of these target compounds exhibited potent protective capacities against glutamate-induced cell damage in SH-SY5Y cells, with compound **9d** being particularly effective. Furthermore, in subsequent experiments, compound **9d** displayed weak hERG inhibitory activity, showing a prolonged lifetime of mice in the hypoxia tolerance model *in vivo* and exhibiting a trend toward reducing the infarct area in the MCAO model. These promising results suggest that compound **9d** may be a valuable candidate for neuroprotection worthy of in-depth study. Additional mechanistic studies and pharmaceutical evaluations of compound **9d** are currently underway and will be reported in due course.

Table 2 *In vitro* and *in vivo* data for selected compounds

Compd.	hERG IC_{50}[a] (μmol/L)	Hypoxia tolerance assay[b], survival time (second)
		20 mg/kg
9d	24.61	4,819.0 ± 1,041.2
Fenazinel	8.64	5,678.0 ± 1,465.6
Control (2% DMSO)	–	3,803.4 ± 780.3

[a]hERG Patch clamp screen as described in Dubin et al.[26] IC_{50} values represent the concentration to inhibit 50% of hERG current (IKr). Numbers represent IC_{50} values generated from 3-point concentration–response relationships in duplicate.
[b]Hypoxia tolerance assay in mice as described in Wang et al.[6]

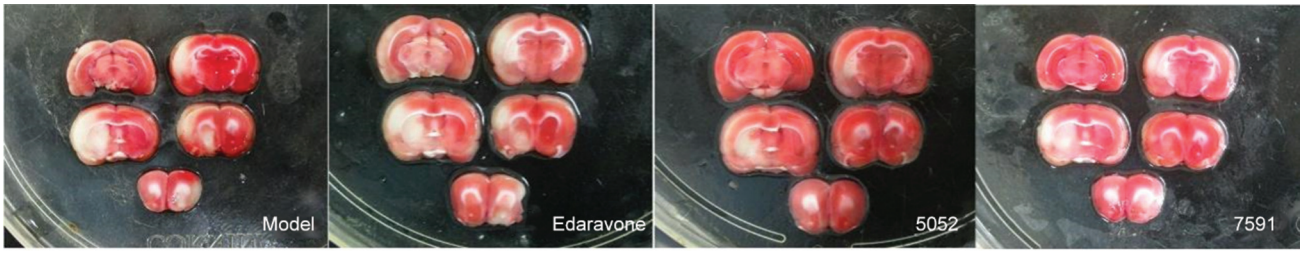

Fig. 3 Effects of test compounds after intraperitoneal injection of 5 mg/kg on the area of cerebral infarction in rats with cerebral ischemia-reperfusion model. "Model" represents the model group; "Edaravone" and "5052" represent positive control groups.

Experimental Section

Reagents and Materials

Unless otherwise specified, all reagents and solvents were purchased from commercial sources (Bidepharm Inc.; Aladdin Inc.; Tansoole Inc., and Sigma-Aldrich) and used without further purification. All air-sensitive reactions were performed under an atmosphere of argon with magnetic stirring. ^{1}H nuclear magnetic resonance (NMR) and ^{13}C NMR spectra were collected on Bruker AVANCE III spectrometers in $CDCl_3$, DMSO-d_6, and d_4-methanol. Chemical shifts were reported as values in parts per million (ppm). The reference resonance peaks were set at 7.26 ppm ($CHCl_3$), 2.50 ppm [$(CD_2H)_2SO$], and 3.31 ppm (CD_2HOD) for ^{1}H NMR spectra and at 77.23 ppm ($CDCl_3$), 39.52 ppm (DMSO-d_6), and 49.00 ppm (CD_3OD) for ^{13}C NMR spectra. Low-resolution mass spectra were determined on an Agilent triple quadrupole mass spectrometer with a 1,220 infinity LC system (HPLC-MS) and an ESI source. Thin-layer chromatography (TLC) was performed on E. Merck precoated silica gel 60 F254 plates with a UV – visible lamp. Column chromatography was performed with Greagent (100 – 400 mesh).

General Synthetic Procedure of intermediate 5a–l

To a solution of substituted benzaldehyde/phenylacetaldehyde (5.0 mmol, 1.0 equiv.) and malonic acid (5.0 mmol, 1.0 equiv.) in pyridine (20 mL) was added piperidine (2 mL). The reaction mixture was stirred at 120°C for 5 hours, at which point TLC indicated that the reaction was complete. After cooling to room temperature, the reaction solution was poured into 50 mL 2N HCl solution to precipitate a white solid. After stirring for 1 hour, the solid was separated by Buchner funnel filtration and washed with water (10 mL × 3) to obtain the crude substitute cinnamic acid **5a**–**l**.

General Synthetic Procedure of Intermediate 7

To a solution of 2-chloroacetyl chloride (36.8 g, 0.25 mol, 1.25 equiv.) and triethylamine (64.5 g, 0.4 mol, 2.0 equiv.) in acetonitrile (80 mL) was added benzylamine (21.43 g, 0.2 mol, 1.0 equiv.) dropwise at 15°C. The reaction mixture was stirred at room temperature for 6 hours. After reaction completion shown by TLC, acetonitrile was evaporated and recrystallized with ethanol/H_2O to afford the desired *N*-benzyl-2-chloroacetamide (18.4 g, yield: 51%).

To a solution of *tert*-butylpiperidin-4-ylcarbamate (20.0 g, 0.1 mol, 1.0 equiv.) in acetone (40 mL) was added *N*-benzyl-2-chloroacetamide (18.4 g, 0.1 mol, 1.0 equiv.), K_2CO_3 (27.6 g, 0.2 mol, 2.0 equiv.), and KI (0.83 g, 5.0 mmol, 0.025 equiv.). The reaction mixture was stirred at 40°C for 6 hours. The reaction solution was cooled to room temperature, filtered, and concentrated under reduced pressure to obtain intermediate **6** (32.5 g, yield: 93.6%).

To a solution of intermediate **6** (32.5 g, 0.09 mol) in ethyl acetate (80 mL) was added HCl at ethyl acetate solution to pH 3 to 4. After stirring at 21°C for 1 hour, the solid was separated by Buchner funnel filtration and washed with ethyl acetate (10 mL) to afford the desired intermediate **7** (27.9 g, yield: 93.1%).

General Synthetic Procedure of 9a–9l

A solution of substituted cinnamic acid **5a**–**5l** (5.0 mmol, 1.0 equiv.) and HBTU (5.5 mmol, 1.1 equiv.) in *N*,*N*-dimethylformamide (50 mL) was stirred at room temperature for 1 hour. And then, to the mixture solution was added intermediate **7** (5.0 mmol, 1.0 equiv.) and triethylamine (15.0 mmol, 3.0 equiv.) dropwise. After stirring at room temperature for 6 hours, the reaction droplets were slowly added to ice-cold water (50 mL) to precipitate the white solid and then stirred for 1 hour. The solid was separated by Buchner funnel filtration and washed with diethyl ether (10 mL × 3). After drying, methanol recrystallization, and hydrochloric acid salt formation, the target compound **9a–9l** was obtained.

General Synthetic Procedure of 9m

To a solution of 1-*tert*-butylcarbonyl piperazine (20.0 g, 0.1 mol, 1.0 equiv.) in acetone (100 mL) was added *N*-benzyl-2-chloroacetamide (18.4 g, 0.1 mol, 1.0 equiv.), K_2CO_3 (27.6 g, 0.2 mol, 2.0 equiv.), and KI (0.83 g, 5.0 mmol, 0.05 equiv.). The reaction mixture was stirred at 40°C for 6 hours. After completion, the reaction solution was cooled to room temperature, filtered, and concentrated under reduced pressure to obtain intermediate **10** (31.9 g, yield: 89.1%).

To a solution of intermediate **10** (31.9 g, 0.09 mol) in ethyl acetate (100 mL) was added HCl at ethyl acetate solution to pH 3 to 4. After stirring at 21°C for 1 hour, the solid was separated by Buchner funnel filtration and washed with ethyl acetate (10 mL) to afford the desired intermediate **11** (26.29 g, yield: 89.7%).

A solution of *p*-methoxycinnamic acid (5.0 mmol, 1.0 equiv.) and HBTU (5.5 mmol, 1.1 equiv.) in *N*,*N*-dimethylformamide (50 mL) was stirred at room temperature for 1 hour. Then, intermediate **7** (5.0 mmol, 1.0 equiv.) and triethylamine (TEA, 15.0 mmol, 3.0 equiv.) were added dropwise. After stirring at room temperature for 6 hours, the reaction droplets were slowly

added to ice-cold water (50 mL) to precipitate the white solid and then continued stirring for 1 hour. The solid was separated by Buchner funnel filtration, washed with diethyl ether (10 mL × 3), and dried to obtain intermediate **12**. After hydrochloric acid salt formation, the target compound **9m** was obtained (1.02 g, 91.4%).

(*E*)-*N*-(1-(2-(benzylamino)-2-oxoethyl)piperidin-4-yl)-3-(4-methoxyphenyl)acrylamide hydrochloride (9a): yield: 85.5%. mp: 256.7–257.5°C. ESI-MS (*m/z*): calcd. for $[M+H]^+$ 408.2209; found 408.33. ^{1}H NMR (400 MHz, DMSO-d_6) δ 10.17 (s, 1H), 8.38 (d, J = 8.0 Hz, 1H), 7.50 (d, J = 12.0 Hz, 2H), 7.41 (s, 1H), 7.37–7.25 (m, 5H), 6.98 (d, J = 8.0 Hz, 2H), 6.53 (d, J = 16.0 Hz, 1H), 4.36 (d, J = 4.0 Hz, 2H), 4.15–4.00 (m, 3H), 3.79 (s, 3H), 3.51 (d, J = 12.0 Hz, 2H), 3.25–3.18 (m, 2H), 2.08–1.98 (m, 2H), 1.88–1.79 (m, 2H).

(*E*)-*N*-(1-(2-(benzylamino)-2-oxoethyl)piperidin-4-yl)-3-(3,4,5-trimethoxyphenyl)acrylamide hydrochloride (9b): yield: 85.8%. mp: 220.0–221.4°C. ESI-MS (*m/z*): calcd. for $[M+H]^+$ 468.2420; found 468.24. ^{1}H NMR (400 MHz, DMSO-d_6) δ 10.08 (s, 1H), 9.25 (t, J = 8.0 Hz, 1H), 8.35 (d, J = 8.0 Hz, 1H), 7.40 (s, 1H), 7.37–7.26 (m, 5H), 6.90 (d, J = 4.0 Hz, 2H), 6.61 (d, J = 16.0 Hz, 1H), 4.36 (d, J = 4.0 Hz, 2H), 4.06–3.99 (m, 3H), 3.81 (s, 6H), 3.68 (s, 3H), 3.52–3.47 (m, 2H), 3.25–3.11 (m, 2H), 1.99 (s, 2H), 1.86–1.78 (m, 2H).

(*E*)-*N*-(1-(2-(benzylamino)-2-oxoethyl)piperidin-4-yl)-3-(3,4-dimethoxyphenyl)acrylamide hydrochloride (9c): yield: 85.3%. mp: 253.8–254.9°C. ESI-MS (*m/z*): calcd. for $[M+H]^+$ 438.2315; found 438.27. ^{1}H NMR (400 MHz, DMSO-d_6) δ 10.06 (s, 1H), 9.23 (d, J = 8.0 Hz, 1H), 8.29 (d, J = 8.0 Hz, 1H), 7.38-7.25 (m, 6H), 7.13 (t, J = 8.0 Hz, 2H), 6.99 (d, J = 8.0 Hz, 1H), 6.53 (d, J = 12.0 Hz, 2H), 4.36 (d, J = 4.0 Hz, 2H), 4.12–3.88 (m, 1H), 3.78 (d, J = 4.0 Hz, 6H), 3.50 (d, J = 12.0 Hz, 2H), 3.20 (q, J = 12.0 Hz, 2H), 2.06–1.98 (m, 2H), 1.85–1.77 (m, 2H).

(*E*)-*N*-(1-(2-(benzylamino)-2-oxoethyl)piperidin-4-yl)-3-(2,3-dimethoxyphenyl)acrylamide hydrochloride (9d): yield: 87.4%. mp: 129.5–132.7°C. ESI-MS (*m/z*): calcd. for $[M+H]^+$ 438.2315; found 438.17. ^{1}H NMR (400 MHz, DMSO-d_6) δ 9.99 (s, 1H), 9.19 (t, J = 8.0 Hz, 1H), 8.41 (d, J = 8.0 Hz, 1H), 7.63 (t, J = 8.0 Hz, 1H), 7.37–7.26 (m, 5H), 7.14–7.06 (m, 3H), 6.67 (d, J = 16.0 Hz, 1H), 4.37 (d, J = 8.0 Hz, 2H), 4.12–3.89 (m, 3H), 3.82 (s, 3H), 3.74 (s, 3H), 3.50–3.35 (m, 2H), 3.24–3.16 (m, 2H), 2.01 (d, J = 16.0 Hz, 2H), 1.85–1.77 (m, 2H).

(*E*)-*N*-(1-(2-(benzylamino)-2-oxoethyl)piperidin-4-yl)-3-(3,5-dimethoxyphenyl)acrylamide hydrochloride (9e): yield: 78.4%. mp: 113.4–115.3°C. ESI-MS (*m/z*): calcd. for $[M+H]^+$ 438.2315; found 438.17. ^{1}H NMR (400 MHz, DMSO-d_6) δ 10.10 (s, 1H), 9.26 (t, J = 4.0 Hz, 1H), 8.42 (d, J = 8.0 Hz, 1H), 7.37 (d, J = 4.0 Hz, 1H), 7.35–7.25 (m, 5H), 6.73 (s, 2H), 6.66 (d, J = 16.0 Hz, 1H), 6.52 (t, J = 4.0 Hz, 1H), 4.36 (d, J = 4.0 Hz, 2H), 4.13–3.89 (m, 3H), 3.77 (s, 6H), 3.50 (d, J = 12.0 Hz, 2H), 3.21 (d, J = 8.0 Hz, 2H), 1.98 (d, J = 4.0 Hz, 2H), 1.87–1.78 (m, 2H).

(*E*)-*N*-(1-(2-(benzylamino)-2-oxoethyl)piperidin-4-yl)-3-(2,4-dimethoxyphenyl)acrylamide hydrochloride (9f): yield: 75.4%. mp: 228.4–230.5°C. ESI-MS (*m/z*): calcd. for $[M+H]^+$ 438.2315; found 438.17. ^{1}H NMR (400 MHz, DMSO-d_6) δ 10.19 (s, 1H), 9.33 (t, J = 8.0 Hz, 1H), 8.32 (d, J = 8.0 Hz, 1H), 7.62–7.56 (m, 1H), 7.44 (t, J = 8.0 Hz, 1H), 7.37–7.25 (m, 5H), 6.61 (t, J = 4.0 Hz, 2H), 6.57 (d, J = 8.0 Hz, 1H), 4.36 (d, J = 4.0 Hz, 2H), 4.13–4.00 (m, 3H), 3.86 (s, 3H), 3.81 (s, 3H), 3.51 (d, J = 12.0 Hz, 2H), 3.26–3.18 (m, 2H), 1.99 (t, J = 8.0 Hz, 2H), 1.88–1.79 (m, 2H).

(*E*)-*N*-(1-(2-(benzylamino)-2-oxoethyl)piperidin-4-yl)-3-(2,5-dimethoxyphenyl)acrylamide hydrochloride (9g): yield: 67.9%. mp: 208.8–209.6°C. ESI-MS (*m/z*): calcd. for $[M+H]^+$ 438.2315; found 438.17. ^{1}H NMR (400 MHz, DMSO-d_6) δ 8.25 (t, J = 8.0 Hz, 1H), 8.03 (d, J = 8.0 Hz, 1H), 7.61 (d, J = 16.0 Hz, 1H), 7.32 (t, J = 8.0 Hz, 2H), 7.26–7.21 (m, 3H), 7.05 (d, J = 4.0 Hz, 1H), 7.00 (d, J = 8.0 Hz, 1H), 6.95–6.92 (m, 1H), 6.86 (d, J = 16.0 Hz, 1H), 4.30 (d, J = 4.0 Hz, 2H), 3.80 (s, 3H), 3.73 (s, 3H), 3.69–3.60 (s, 1H), 2.97 (s, 2H), 2.78 (d, J = 12.0 Hz, 2H), 2.18 (t, J = 8.0 Hz, 2H), 1.77 (d, J = 8.0 Hz, 2H), 1.53–1.45 (m, 2H).

(*E*)-*N*-(1-(2-(benzylamino)-2-oxoethyl)piperidin-4-yl)-3-(3-methoxyphenyl)acrylamide hydrochloride (9h): yield: 77.9%. mp: 203.6–204.4°C. ESI-MS (*m/z*): calcd. for $[M+H]^+$ 408.2209; found 408.2. ^{1}H NMR (400 MHz, DMSO-d_6) δ 10.13 (s, 1H), 9.28 (t, J = 8.0 Hz, 1H), 8.46 (d, J = 8.0 Hz, 1H), 7.41 (d, J = 16.0 Hz, 1H), 7.37–7.25 (m, 6H), 7.13 (d, J = 12.0 Hz, 2H), 6.96 (dd, J = 4.0 Hz, 8.0 Hz, 1H), 6.68 (d, J = 16.0 Hz, 1H), 4.36 (d, J = 4.0 Hz, 2H), 4.15–3.90 (m, 3H), 3.78 (s, 3H), 3.51 (d, J = 12.0 Hz, 2H), 3.21 (d, J = 12.0 Hz, 2H), 2.08–1.99 (m, 2H), 1.88–1.79 (m, 2H).

(*E*)-*N*-(1-(2-(benzylamino)-2-oxoethyl)piperidin-4-yl)-3-(2-methoxyphenyl)acrylamide hydrochloride (9i): yield: 79.1%. mp: 177.4–179.4°C. ESI-MS (*m/z*): calcd. for $[M+H]^+$ 408.2209; found 408.2. ^{1}H NMR (400 MHz, DMSO-d_6) δ 8.25 (t, J = 8.0 Hz, 1H), 8.03 (d, J = 8.0 Hz, 1H), 7.63 (d, J = 12.0 Hz, 1H), 7.50 (d, J = 4.0 Hz, 1H), 7.38–7.34 (m, 3H), 7.26–7.21 (m, 3H), 7.07 (d, J = 8.0 Hz, 1H), 6.98 (t, J = 8.0 Hz, 1H), 6.65 (d, J = 16.0 Hz, 1H), 4.30 (d, J = 4.0 Hz, 2H), 3.85 (s, 3H), 3.66–3.63 (m, 1H), 2.97 (s, 2H), 2.77 (d, J = 12.0 Hz, 2H), 2.17 (t, J = 8.0 Hz, 2H), 1.77 (d, J = 8.0 Hz, 2H), 1.54–1.45 (m, 2H).

(*E*)-*N*-(1-(2-(benzylamino)-2-oxoethyl)piperidin-4-yl)-3-(2,3,4-trimethoxyphenyl)acrylamide hydrochloride (9j): yield: 82.1%. mp: 190.3–192.7°C. ESI-MS (*m/z*): calcd. for $[M+H]^+$ 468.2420; found 468.2. ^{1}H NMR (400MHz, DMSO-d_6) δ 8.25 (t, J = 8.0 Hz, 1H), 8.00 (d, J = 8.0 Hz, 1H), 7.50 (d, J = 16.0 Hz, 1H), 7.34–7.23 (m, 6H), 6.88 (d, J = 8.0 Hz, 1H), 6.57 (d, J = 16.0 Hz, 1H), 4.30 (d, J = 4.0 Hz, 2H), 3.83 (s, 3H), 3.80 (s, 3H), 3.75 (s, 3H), 3.67–3.60 (m, 1H), 2.97 (s, 2H), 2.77 (d, J = 12.0 Hz, 2H), 2.18 (t, J = 8.0 Hz, 2H), 1.77 (d, J = 8.0 Hz, 2H), 1.53–1.45 (m, 2H).

***N*-(1-(2-(benzylamino)-2-oxoethyl)piperidin-4-yl)cinnamamide hydrochloride (9k):** yield: 87.4%. mp: 148.4–149.5°C. ESI-MS (*m/z*): calcd. for $[M+H]^+$ 378.2103; found 378.2. ^{1}H NMR (400 MHz, DMSO-d_6) δ 8.50 (t, J = 8.0 Hz, 2H), 8.25 (t, J = 4.0 Hz, 1H), 8.10 (dd, J = 3.6 Hz, 4.4 Hz, 1H), 7.87–7.85 (m, 1H), 7.32 (t, J = 8.0 Hz, 2H), 7.26–7.22 (m, 6H), 6.29 (d, J = 8.0 Hz, 1H), 4.30 (t, J = 4.0 Hz, 2H), 3.48 (s, 1H), 2.97 (s, 2H), 2.72 (d, J = 4.0 Hz, 2H), 2.21 (t, J = 4.0 Hz, 2H), 1.80 (d, J = 8.0 Hz, 2H), 1.49–1.43 (m, 2H).

(*E*)-*N*-(1-(2-(benzylamino)-2-oxoethyl)piperidin-4-yl)-4-phenylbut-2-enamide hydrochloride (9l): yield: 75.3%.

mp: 162.9–163.3°C. ESI-MS (*m/z*): calcd. for $[M+H]^+$ 392.2260; found 392.2. ^{1}H NMR (400MHz, DMSO-d_6) δ 9.99 (s, 1H), 9.19 (s, 1H), 8.20 (d, $J=8.0$ Hz, 1H), 7.40 (d, $J=8.0$ Hz, 2H), 7.36 -7.21 (m, 8H), 6.45 (d, $J=16.0$ Hz, 1H), 6.36–6.29 (m, 1H), 4.36 (d, $J=8.0$ Hz, 2H), 3.97 (s, 2H), 3.80–3.74 (m, 1H), 3.49–3.41 (m, 2H), 3.14 (s, 2H), 3.05 (d, $J=8.0$ Hz, 2H), 1.94 (d, $J=12.0$ Hz, 2H), 1.76 (q, $J=8.0$ Hz, 2H).

(*E*)-*N*-benzyl-2-(4-(3-(4-methoxyphenyl)acryloyl) piperazin-1-yl)acetamide hydrochloride (9m): yield: 91.4%. mp: 237.6–239.5°C. ESI-MS (*m/z*): calcd. for $[M+H]^+$ 394.2052; found 394.2. ^{1}H NMR (400 MHz, DMSO-d_6) δ 10.48 (s, 1H), 9.17 (s, 1H), 7.69 (d, $J=8.0$ Hz, 2H), 7.51 (d, $J=16.0$ Hz, 1H), 7.37–7.26 (m, 5H), 7.14 (d, $J=16.0$ Hz, 1H), 6.98 (d, $J=8.0$ Hz, 2H), 4.53 (s, 2H), 4.37 (d, $J=8.0$ Hz, 2H), 4.06 (s, 2H), 3.80 (s, 3H), 3.54 (s, 3H), 3.16 (s, 3H).

Neuroprotection Assay against Glu-Induced Cell Damage in SH-SY5Y Cells

Cortical Neuron Culture

Postnatal 1-day-old Sprague-Dawley (SD) Suckling rats (Sipu-BiKAI, SCXK2008–0016) were decapitated under sterile conditions in an ultra-clean table, and bilateral cortices were collected in ice-cold D-Hanks solution (Boster) with a curved forceps. The meninges, blood vessels, and other tissues were carefully removed, and the tissue was cut to 1 mm^3 by iris scissors. Then, an appropriate amount of trypsin (0.125%) was added and digested at 37°C for 20 minutes. The trypsin was discarded, and the whole culture solution (DMEM [Corning Cellgro] containing 10% serum [Pufei]) was added for 5 minutes to terminate the effect of trypsin. After centrifugation at 800 rpm for 5 minutes, the supernatant was discarded and 1 mL of culture medium was added, filtered through a 75 µm filter membrane, counted, and resuspended to make a uniform density single cell suspension (10^5–2×10^5 cells/mL). The single cell suspension was seeded in a 96-well plate coated with polylysine (Sigma), 200 µL per well, and was cultured in a 5% CO_2 incubator at 37°C. After 24 hours, the cells were changed to maintenance medium [96% Neurobasal (Gibo) + 2% B27 (Gibo) + 1% L-Glutamax (Gibo) + 1% Gentamicin-streptomycin (Boster)], and then the medium was changed every 3 days.

Glutamate Treatment

Primary cultured cells were divided into a normal culture group, model group, drug treatment group, and positive control group (for primary screening compounds screening mode was 2 concentrations gradients [1, 10 µmol/L], 2 multiple holes; for the further screening compound, the concentration gradient was 10, 20, 50, 100 µmol/L, 3 multiple holes). For neurons cultured to day 10 to 12, the original culture medium was aspirated and DMEM medium without serum was added. Except for the normal group and the model group, each drug group was pretreated with different concentrations of the test substance for 0.5 hours and then incubated with 300 µmol/L glutamate for 24 hours. MTT assay was performed 24 hours later to determine cell viability. Specifically, 5 mg/mL MTT solution (Sigma) was added to each well to achieve a final concentration of 0.5 mg/mL, and the culture was continued in the CO_2 incubator (Heraeus) for 4 hours. Then, the culture solution was abandoned and 200 µL DMSO was added to each well, and the optical density (OD) value (measuring at 570 nm) was read on a microplate reader (Labsystem Dragon). The following formula was used:

Cell rate (%) = (OD values of the treated groups − OD value of the model group)/(OD values of the normal groups − OD value of the model group) × 100%.

All data were presented as mean ± standard error. For each batch of experiments, only the mean and standard deviation of each compound hole under the same treatment condition were listed, without statistical comparison. Rigorous statistical comparisons require at least three independent batches of experiments.

Hypoxia Tolerance Assay

A total of 30 male ICR (Institute of Cancer Research) mice (Sipu-BiKAI, SCXK2008–0016), weighing 18 to 20 g, were divided into three groups: DMSO control group, Fenazinel, **9d** in the dose of 20 mg/kg (10 animals per group). The injection volume was 0.1 mL/10 g. After the mice were injected with each sample through the tail vein, the mice in each group were placed in 250 mL grinding mouth bottles containing 5 g sodium lime (1 mouse per bottle), capped, and sealed. The respiratory arrest was taken as an indication of death, and the survival time of the mice was observed. The *t*-test was used for statistical analysis, and all data were expressed as mean ± standard deviation.

hERG Inhibitory Activity Assay

Cell Culture Preparation

CHO-hERG cells were cultured in 175 cm^2 culture flasks, and when the cell density had grown to 60 to 80%, the culture medium was removed, washed once with 7 mL phosphate-buffered saline, and then digested with 3 mL Detachin. After complete digestion, add 7 mL culture medium to neutralization, then centrifugation, suction up to the supernatant, and add 5 mL culture medium to resuspension, to ensure the cell density of 2–5 $\times10^6$ /mL.

Electrophysiological Recording Process

The single-cell high-impedance sealing and whole-cell pattern formation processes were all performed automatically by the Qpatch instrument. After the whole-cell recording mode was obtained, the cell was clamped at −80 mV, followed by a 50 millisecond prevoltage of −50 mV before a 5-second +40 mV depolarization stimulus, and then repolarized to −50 mV for 5 seconds. Then go back to −80 millivolts. This voltage stimulus was applied every 15 seconds and recorded for 2 minutes followed by 5 minutes of extracellular fluid recording and then the administration process was started. The compound concentration was 40, 13.33, 4.44, 1.48, 0.49, and 0.16 µmol/L, respectively, starting from the lowest tested concentration. Each test concentration was administered for 2.5 minutes, and after all, concentrations

were administered consecutively, and the positive control compound 3 μmol/L Fenazinel was administered. At least three cells ($n \geq 3$) were tested for each concentration.

MCAO-Induced Cerebral Ischemia/Reperfusion Injury Model

Pharmacological studies were performed by the Center for Pharmacological Evaluation and Research according to protocols approved by the Animal Care and Use Committee of the Shanghai Institute of Pharmaceutical Industry. All experiments are reported in compliance with the ARRIVE (Animal Research: Reporting *in vivo* Experiments) guidelines. Healthy male SD rats were divided into four groups, namely, model group, compound 7591 (5 mg/kg), Fenazinel/5052 (5 mg/kg), and Edaravone (5 mg/kg). The rats were anesthetized by intraperitoneal injection of 12% chloral hydrate (360 mg/kg) and fixed on the operating table supine. The nylon thread with a diameter of 0.26 mm and a length of 20 mm entered from the external carotid artery to the proximal end of the anterior cerebral artery. All blood flow sources of the MCA were blocked. Then, 1.5 hours later, the nylon thread was pulled out to re-flow the blood. The rats were intraperitoneally injected test samples and raised in separate cages.

The rats were sacrificed 24 hours after administration. Their brains were taken and on average cut into five slices. Then, pathological sections were placed in TTC solution and incubated at 37°C for 5 to 10 minutes for staining. The infarct area is not colored, and the normal brain tissue is stained red.

Conflict of Interest
None declared.

Acknowledgments
We gratefully acknowledge financial support from the National Science and Technology Major Project (Grant No. 2018ZX09711002-002-009), the National Natural Science Foundation of China (Grant No. 81703358), the Science and Technology Commission of Shanghai Municipality (Grant Nos. 17431903900, 18QB1404200, 21S11908000, 22ZR1460300), and the Graduate Innovation Fund Project of China State Institute of Pharmaceutical Industry (Grant Nos. YJS2021013, YJS2021011).

Reference

1 Kunt R, Çınar BP, Yüksel B, et al. Clinical-epidemiological and radiological characteristics of stroke patients: a multicentre study. Int J Clin Pract 2021;75(12):e14963
2 Wu LQ. Pharmacologic treatment of ischemic stroke [in Chinese]. Prog Pharm Sci 2003;27(05):303–306
3 Huber CC, Wang X, Wang H. Impact of cardiovascular diseases on ischemic stroke outcomes. J Integr Neurosci 2022;21(05):138
4 Zhang QW, Jiang L, Wang G, Li JQ. Design, synthesis and neuroprotective effects of fenazinel derivatives. Chin Chem Lett 2017; 28(07):1505–1508
5 Li J, Huang L, Xia Y. Synthesis of aroylpiperazine derivatives and their anti-cerebral anoxia, anti-cerebral ischemia biological activities. Zhongguo Yaowu Huaxue Zazhi 2006;16(01):6–14
6 Wang WY, Shen CW, Weng ZJ, et al. Design, synthesis and biological evaluation of novel dicarbonylalkyl piperazine derivatives as neuroprotective agents. Chin Chem Lett 2016;27(03):387–390
7 Zhao T. Protective effects of fenazinel dihydrochloride against stroke in stroke-prone spontaneously hypertensive rats. Acad J Second Military Med Univ 2011:1282–1285
8 Li D, Li J, Huang L. Protective effects of fenazinel dihydrochloride on focal cerebral ischemic injury in rats. Chin Pharmacol Bull 2009;25:716–720
9 Jin L, Sheng Y, Zhong Y, Zhu P, Xia Y. Relation between therapeutic effects and administration time of fenazinel dihydrochloride on focal cerebral ischemia injury in rats. Carol J Pharm 2008;5:356–358
10 Chen Y, Lu M, Zhang B, Xie B. Preparation of fenazinel dihydrochloride injection. Carol J Pharm 2007;38(12):852–854
11 Recanatini M, Poluzzi E, Masetti M, Cavalli A, De Ponti F. QT prolongation through hERG K(+) channel blockade: current knowledge and strategies for the early prediction during drug development. Med Res Rev 2005;25(02):133–166
12 Zhang X, He X, Chen Q, Lu J, Rapposelli S, Pi R. A review on the hybrids of hydroxycinnamic acid as multi-target-directed ligands against Alzheimer's disease. Bioorg Med Chem 2018;26(03):543–550
13 Villareal MO, Sasaki K, Margout D, et al. Neuroprotective effect of Picholine virgin olive oil and its hydroxycinnamic acids component against β-amyloid-induced toxicity in SH-SY5Y neurotypic cells. Cytotechnology 2016;68(06):2567–2578
14 Wang K, Shi J, Zhou Y, et al. Design, synthesis and evaluation of cinnamic acid hybrids as multi-target-directed agents for the treatment of Alzheimer's disease. Bioorg Chem 2021;112:104879
15 Ojha S, Javed H, Azimullah S, Abul Khair SB, Haque ME. Neuroprotective potential of ferulic acid in the rotenone model of Parkinson's disease. Drug Des Devel Ther 2015;9:5499–5510
16 Yoon BH, Jung JW, Lee JJ, et al. Anxiolytic-like effects of sinapic acid in mice. Life Sci 2007;81(03):234–240
17 Lee EH, Shin JH, Kim SS, Seo SR. Sinapic acid controls inflammation by suppressing nlrp3 inflammasome activation. Cells 2021; 10(09):2327
18 Płowuszyńska A, Gliszczyńska A. Recent developments in therapeutic and nutraceutical applications of *p*-methoxycinnamic acid from plant origin. Molecules 2021;26(13):3827
19 Rychlicka M, Rot A, Gliszczyńska A. Biological properties, health benefits and enzymatic modifications of dietary methoxylated derivatives of cinnamic acid. Foods 2021;10(06):1417
20 He L, Du JJ, Zhou JJ, et al. Synthesis of melatonin derivatives and the neuroprotective effects on parkinson's disease models of caenorhabditis elegans. Front Chem 2022;10:918116
21 Sevindik M, Akgul H, Selamoglu Z, Braidy N. Antioxidant, antimicrobial and neuroprotective effects of Octaviania asterosperma in vitro. Mycology 2020;12(02):128–138
22 Zhang L, Wu Y, Yang G, et al. Design, synthesis and biological evaluation of novel osthole-based derivatives as potential neuroprotective agents. Bioorg Med Chem Lett 2020;30(24):127633
23 Lu T, Liu Y, Liu Y, et al. Discovery, biological evaluation and molecular dynamic simulations of butyrylcholinesterase inhibitors through structure-based pharmacophore virtual screening. Future Med Chem 2021;13(09):769–784
24 Cifuentes J, Salazar VA, Cuellar M, et al. Antioxidant and neuroprotective properties of non-centrifugal cane sugar and other sugarcane derivatives in an in vitro induced parkinson's model. Antioxidants 2021;10(07):1040
25 Petrovic N, Tosti T, Srbljak I, Đurić A, Kosanic M. Chemical composition and bioctivity of the giant polypore or black-staining mushroom, meripilus giganteus (agaricomycetes), from serbia. Int J Med Mushrooms 2022;24(07):21–40
26 Dubin AE, Nasser N, Rohrbacher J, et al. Identifying modulators of hERG channel activity using the PatchXpress planar patch clamp. J Biomol Screen 2005;10(02):168–181